



Article

Estimating Evapotranspiration of Greenhouse Tomato under Different Irrigation Levels Using a Modified Dual Crop Coefficient Model in Northeast China

Mingze Yao ¹, Manman Gao ², Jingkuan Wang ^{1,*}, Bo Li ², Lizhen Mao ³, Mingyu Zhao ⁴, Zhanyang Xu ², Hongfei Niu ⁵, Tieliang Wang ², Lei Sun ² and Dongshuang Niu ²

¹ College of Land and Environment, Shenyang Agricultural University, Shenyang 110866, China; yaomingze@syau.edu.cn

² College of Water Conservancy, Shenyang Agricultural University, Shenyang 110866, China; gmm15066234536@163.com (M.G.); liboshuili@syau.edu.cn (B.L.); 1989500008@syau.edu.cn (T.W.); ssunleiii@163.com (L.S.); a15943606929@163.com (D.N.)

³ Department of Foreign Languages Teaching, Shenyang Agricultural University, Shenyang 110866, China; fszmlz@126.com

⁴ College of Energy and Water Resources, Shenyang Institute of Technology, Fushun 113122, China; zhaomingyu@situ.edu.cn

⁵ College of Hydraulic Engineering, Liaoning Vocational College of Ecological Engineering, Shenyang 110122, China; crystallove202707@126.com

* Correspondence: jkwang@syau.edu.cn

Abstract: Accurate quantification of evapotranspiration (ET_c) and its components are critical for enhancing water use efficiency and implementing precision irrigation. A two-year experiment was conducted for greenhouse-grown tomatoes under mulched drip irrigation with three irrigation treatments during 2020–2021 in Northeast China. Three different irrigation treatments were applied by setting upper and lower soil moisture irrigation thresholds (i.e., W1, $65\%\theta_{FC}-75\%\theta_{FC}$, W2, $75\%\theta_{FC}-85\%\theta_{FC}$, W3, $85\%\theta_{FC}-95\%\theta_{FC}$, respectively, where θ_{FC} is field capacity). In this study, a modified dual crop coefficient (K_c) model was proposed to simulate daily ET_c , plant transpiration (T_r) and soil evaporation (E_s). The simulations of the model were validated against observed data from the sap flow system combined with the soil water balance method. The controlling factors on the variations of evapotranspiration and its components were also identified by using the path analysis method. Results showed that the modified dual K_c model can accurately simulate daily ET_c , E_s , and T_r for the greenhouse tomato under different irrigation conditions, with the coefficients of determination ranging from 0.88 to 0.98 and the index of agreement higher than 0.90. The seasonal cumulative ET_c of tomato for W1–W3 were 138.5–194.4 mm, of which 9.5–15.8% was consumed by E_s . Path analysis showed that the net radiation (R_n) was the dominant factor controlling the variations of T_r and ET_c during the growing seasons. The canopy coverage degree (K_{cc}) was the dominant controlling factor of E_s , while the temperature (T_a) was the primary limiting factor affecting E_s . This study can provide reference information for developing proper irrigation management in a greenhouse-grown tomato in the north cold climate regions.

Keywords: modified dual crop coefficient model; crop coefficients; evapotranspiration partition; controlling factors



Citation: Yao, M.; Gao, M.; Wang, J.; Li, B.; Mao, L.; Zhao, M.; Xu, Z.; Niu, H.; Wang, T.; Sun, L.; et al. Estimating Evapotranspiration of Greenhouse Tomato under Different Irrigation Levels Using a Modified Dual Crop Coefficient Model in Northeast China. *Agriculture* **2023**, *13*, 1741. <https://doi.org/10.3390/agriculture13091741>

Academic Editor: Yanqun Zhang

Received: 29 July 2023

Revised: 30 August 2023

Accepted: 30 August 2023

Published: 1 September 2023



Copyright: © 2023 by the authors. Licensee MDPI, Basel, Switzerland. This article is an open access article distributed under the terms and conditions of the Creative Commons Attribution (CC BY) license (<https://creativecommons.org/licenses/by/4.0/>).

1. Introduction

Solar greenhouse is a technique to ensure the sustainable production of vegetables and has been widely used worldwide [1]. The total area of greenhouses in 2018 was 1.89×10^6 hectares, according to the Ministry of Agricultural Mechanization Statistics. Tomato (*Lycopersicon esculentum* Mill.) is one of the major vegetables grown in solar greenhouse [2]. Currently, the irrigation scheduling for a greenhouse is typically based on the

experience of the farmer, which generally leads to production quality loss, plant disease susceptibility, and low water use efficiency [3,4]. Crop evapotranspiration (ET_c) is an important basis for optimizing the irrigation water management strategy and enhancing crop water productivity [5]. The ET_c can be divided into plant transpiration (T_r) and soil evaporation (E_s). However, the functions of E_s and T_r are different within the agriculture system. T_r is associated with plant growth and productivity, playing an important role in photosynthesis and dry matter accumulation in crops [6]. Conversely, E_s is generally considered to be ineffective in water consumption and should be reduced as much as possible by crop management practices [7–9]. Therefore, it is crucial to accurately determine ET_c and its components for attaining efficient irrigation scheduling and enhancing water use efficiency.

The crop ET_c is mainly obtained by direct measurement or numerical simulation. The water balance method [10], weighing lysimeter [11], and micro-lysimeter plus sap flow system are common instruments for measuring ET_c of crops in different climate regions [12]. The direct measurements of ET_c are costly and laborious; thus, many models have become the main tool to estimate ET_c . The most commonly used models include the Penman–Monteith (PM) model [13], Priestley–Taylor model [5], Shuttle–Wallace model [14] and crop coefficient (K_c) model [15,16]. Among them, the dual crop coefficient (K_c) model has been extensively applied to estimate the components of ET_c with its practical simplicity and robustness [17–19]. The dual K_c model can divide K_c into basal crop coefficient (K_{cb}) and soil evaporation coefficient (K_e), characterizing plant transpiration and soil evaporation, respectively. This model further considers the effect of inadequate soil water on crop ET_c using a water stress coefficient (K_s) [20,21]. The dual K_c method has been successfully used for various crops grown in greenhouses or open fields [17,22–24].

The performance of the dual K_c model mainly depends on the precise determination of crop coefficient values and accurate estimation of reference evapotranspiration (ET_o) [8,21,22]. As K_{cb} and K_e values vary at different stages of crop growth that are affected by meteorological conditions, crop characteristics, and management practices, researchers thus need to identify the dynamic values of K_{cb} and K_e in accordance with local conditions [16,18,21,25]. For example, Ding et al. [25] developed an improved dual K_c model by introducing canopy coverage coefficient (K_{cc}) to calculate dynamic daily K_{cb} . Yan et al. [26] modified K_{cb} and K_e for cucumber plants by applying measured meteorological data, leaf area index (LAI), and soil moisture content (SWC) in a Venlo-type greenhouse. In Northeast China, cultivated tomatoes in greenhouses are mainly subjected to low air temperature conditions during cold seasons [27]. The plant temperature constraint (f_t) could lead to the reduction of stomatal opening, which, in turn, inhibits crop transpiration and reduces ET_c [5]. Although there have been some dynamic dual K_c models, these models rarely consider the effect of the plant temperature constraint on T_r , which could result in an inaccurate estimation of ET_c . In addition, irrigation level is also an important factor in estimating evapotranspiration; several studies showed that ET_c has an increasing trend with the increase in irrigation amount [11,28,29]. However, applying the dual K_c model to quantify ET_c and its component of greenhouse tomatoes under different irrigation conditions is still limited.

Evapotranspiration participates in the exchange of energy and water vapor between the surface and the atmosphere [5,12]; hence, knowledge of the factors controlling changes in evapotranspiration is essential for improving the microclimate environment conditions of crops. Previous studies revealed that ET_c is influenced by multiple interactions among canopy structure, soil moisture status, and meteorological conditions [12,30], but T_r and E_s respond differently to these biological and abiotic factors because of the different water consumption mechanisms [31]. In addition, the dominant factors affecting ET_c and its components may be different in different regions and climates. For instance, Gong et al. [11] showed that net radiation was the dominant meteorological factor affecting ET_c for greenhouse tomatoes in the North China Plain. However, Granier et al. [32] reported that T_r was primarily controlled by water vapor pressure deficit and had little relationship with solar radiation in the climate of tropical rainforest regions. Therefore, there is a need to

investigate how different factors mediate ET_c components of greenhouse tomatoes and what are the main controlling factors in the cold region of Northeast China.

Above all, the main objectives of the present study are: (1) investigate the dynamic variations in f_t , K_{cb} , K_e , and K_s under different irrigation levels; (2) develop the modified dual K_c model and evaluate the applicability of the model for simulating ET_c and its components of greenhouse tomatoes under different irrigation levels; (3) analyze the seasonal variations of ET_c and its components, and quantify T_r , E_s and ET_c of greenhouse tomatoes under different irrigation treatments at different growth stage; (4) identify the dominant controlling factors on daily evapotranspiration and its components of greenhouse tomatoes.

2. Materials and Methods

2.1. Experimental Site and Design

The experiment was conducted using tomato plants in a solar greenhouse at No. 43 Experimental Station of Shenyang Agricultural University ($41^{\circ}82' N$, $123^{\circ}57' E$, Figure 1a) from August to December in 2020 and 2021. The study area is in a continental monsoon climate with an average annual air temperature of $8^{\circ}C$, a mean annual precipitation of 799 mm, and the frost-free period lasts for over 150 d. The greenhouse is 70 m in length \times 8 m span and 4 m in ridge height, oriented in the east–west direction. The greenhouse adopts a single-sided daylighting parabolic type structure, which regulates interior temperature and humidity through ventilation openings on the roof and bottom during daytime. In addition, the rain-proof quilt is spread on the surface of the shed film to maintain the temperature at night in winter. The soil texture was brown loam soil with an average bulk density of $1.26 g/cm^3$, field capacity (θ_{FC}) of $0.31 cm^3 cm^{-3}$, and permanent wilting point (θ_{WP}) of $0.09 cm^3 cm^{-3}$ in a depth of 0–60 cm.

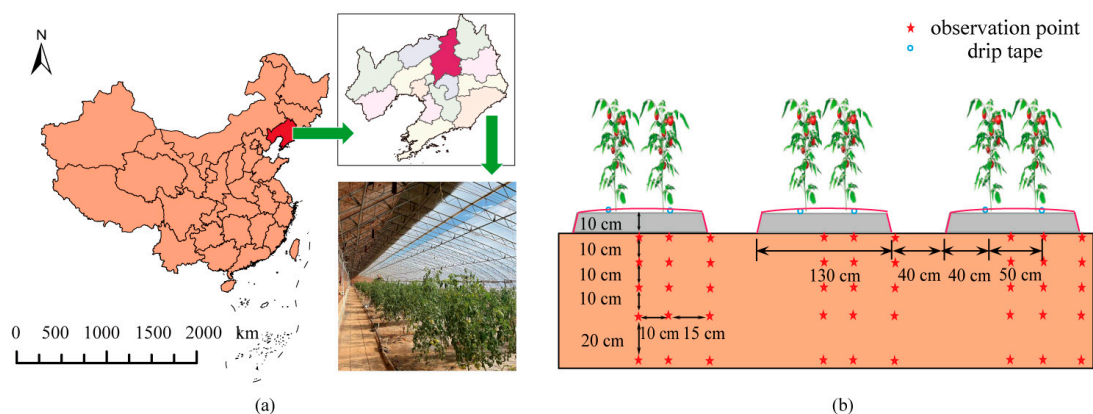


Figure 1. (a) The location of the study areas; (b) Placement of tomato plants and layout of drip irrigation system.

The experiment used a completely random design comprising three replicates of three treatments for a total of nine plots, each plot consisting of two rows of thirty-two tomato plants. The mulched drip irrigation was adopted in this experiment. In order to prevent lateral soil water exchange between two neighboring plots, an impermeable plastic film was embedded vertically in the soil to a depth of 100 cm. All tomato plants were fully irrigated at the initial stage to ensure plant survival; thereafter, the three irrigation treatments (W1, $65\%\theta_{FC}$ – $75\%\theta_{FC}$, W2, $75\%\theta_{FC}$ – $85\%\theta_{FC}$, W3, $85\%\theta_{FC}$ – $95\%\theta_{FC}$, respectively) were applied on the plants referencing to the previous studies. Irrigation scheduling was determined by the set upper and lower irrigation limits, which were based on an automatic drip irrigation system. Each drip irrigation event was automatically controlled via a solenoid valve when the soil water content reached the defined irrigation trigger thresholds. The pressure-compensated emitters were applied for the experiment with a discharge rate of $1.6 L h^{-1}$ and emitter spacing of 0.4 m. A local widely used variety of tomato plant (Fenguan No.1) was planted with a row spacing of 0.5 m and a plant spacing

of 0.4 m. The design of tomato planting and drip pipe arrangement follows the “one film, two pipes and two rows of tomato arrangement”. The width and spatial interval of the plastic mulches were 1.3 m and 0.4 m, respectively (Figure 1b). Tomatoes were transplanted on August 14 and August 11 and harvested on 13 December and 8 December in 2020 and 2021, respectively. The tomato growth stages in each season were divided into four stages according to Allen et al. [21] and local observations. The detailed dates and the irrigation amount of each plant growing stages in two seasons are documented, as shown in Table 1.

Table 1. Growth dates and irrigation water amounts of the greenhouse tomatoes in 2020 and 2021.

Year	Growth Stage	Date	Irrigation Amount (mm)		
			W1	W2	W3
2020	Initial	8.14–9.07	21.2	21.8	23.0
	Development	9.08–10.09	31.9	37.2	46.2
	Middle	10.10–11.11	47.1	59.3	76.5
	Late	11.12–12.13	18.8	27.8	35.3
2021	Initial	8.11–9.01	25.2	24.9	25.7
	Development	9.02–10.05	33.4	42.1	47.6
	Middle	10.06–11.06	49.5	63.4	74.2
	Late	11.07–12.08	19.5	26.2	32.3

2.2. Measurements and Methods

An automatic weather station (HOBO, Onset, Bourne, MA, USA) was used to continuously monitor the air temperature (T_a), relative humidity (RH), solar radiation, and other meteorological data in the greenhouse. The net radiation (R_n) was measured by a net radiometer (NR LITE2, Kipp & Zonen, Delft, The Netherlands) at 2 m above the ground. The air velocity (u) was measured by a three-dimensional anemometer sensor (CSAT-3, Campbell Scientific, Inc., Logan, UT, USA) at the same height. All the data were recorded by a CR1000 data logger (Campbell Scientific, Inc., Logan, UT, USA) every 30 min. The vapor pressure deficit (VPD) was further calculated from T_a and RH according to FAO 56 [21].

The volumetric soil water contents (SWC) were monitored by the Campbell water monitoring system every 10 min. Soil moisture probes were buried below the dropper, in the furrow, and in the middle of the ridge at depths of 10, 20, 30, 40, and 60 cm. The soil water contents were calibrated using the overdrying method during the growth season. The average soil water content at 0–60 cm depth for different irrigation water treatments is shown in Figure 2.

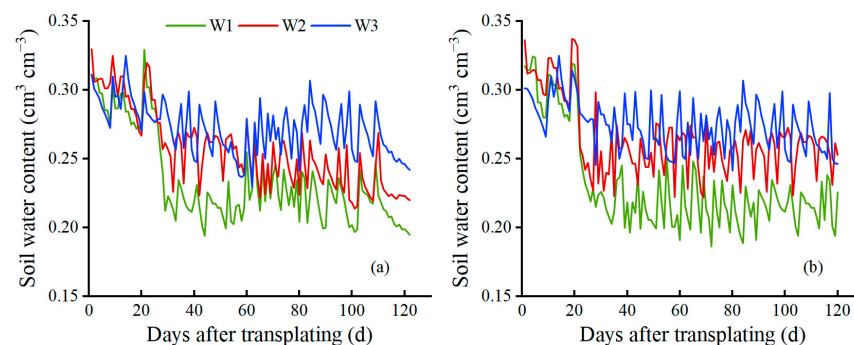


Figure 2. The variations of average soil water content at 0–60 cm depth during tomato growing season in 2020 (a) and 2021 (b) under different irrigation treatments.

The plant height and leaf area index (LAI) were measured every 7–10 days with four replications in each treatment. The tomato height was measured using a measuring tape. LAI was measured with an LAI-2200C plant canopy analyzer (LI-COR, Lincoln, NE, USA), and the details of the operating procedures can be found in the references [33,34]. In addition, to obtain the daily tomato height and LAI, the plant height and LAI simulations were

fitted by the logistic model [35] and the growth curve equation proposed by Ding et al. [36]. As shown in Figure 3, the R^2 values of the two crop growth models were all higher than 0.98, which illustrated that both models had a good performance in fitting the daily tomato plant height and LAI.

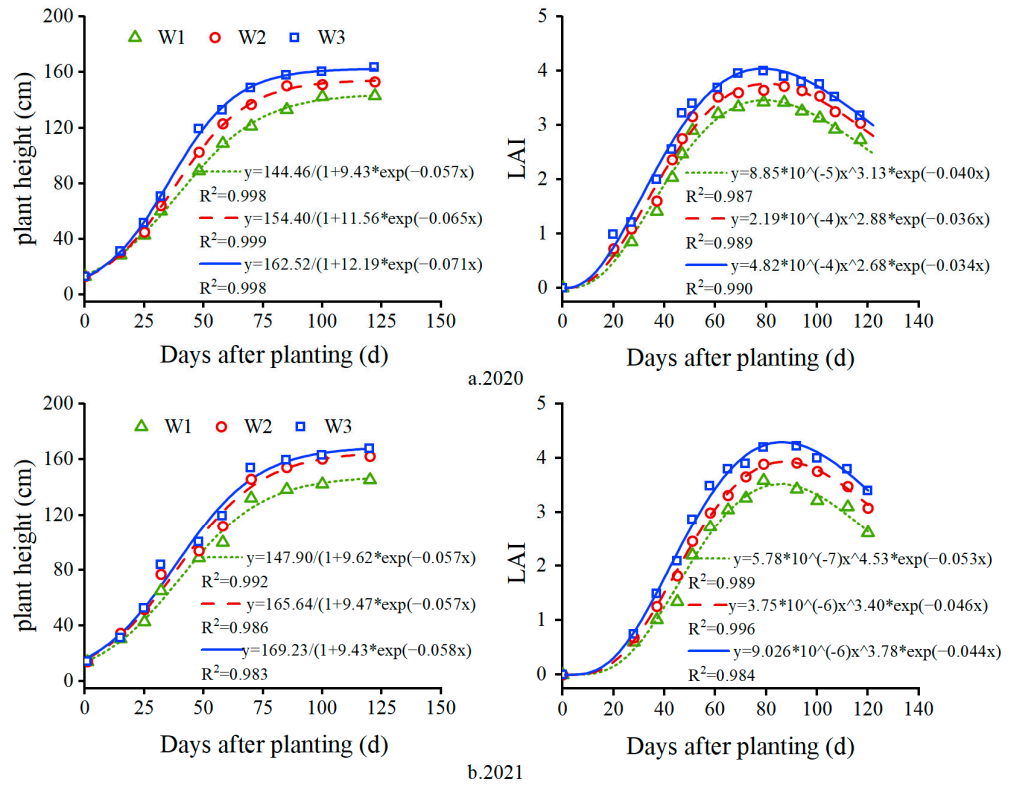


Figure 3. Simulation of plant height and leaf area index (LAI) under different irrigation treatments during greenhouse tomato growth period in 2020 and 2021.

The logistic equation is as follows [37]:

$$h = a / (1 + b \times \exp(-c \times x)) \tag{1}$$

where x is the days after planting; a , b , and c are fitted parameters; a is the upper limit of tomato height.

The LAI growth curve equation is as follows [31,36]:

$$\text{LAI} = d \times x^f \times \exp(-r \times x) \tag{2}$$

where d , f , and r are fitted parameters, and r is the LAI change rate.

Four representative tomato plants were randomly selected from each treatment for the measurement of sap flow rate with a wrapped sensor (Flow32-1k system, Dynamax, USA) during the crop development, middle, and late stages. The sensors were installed 20 cm above the ground and wrapped with aluminum foil to minimize heat from direct radiation. More installations and measurement details were referred to Steinberg et al. [38]. The sap flow data were collected every 30 min using a data logger. The tomato transpiration could be calculated as [39]:

$$T_r = \frac{1}{1000} \left[\sum_{i=1}^n \frac{f_i / LA_i}{n} \right] \text{LAI} \tag{3}$$

where T_r is the transpiration rate of tomato (mm d^{-1}); n is the sampling number; f_i is the measured stem flow (g/d); LA_i is the leaf area (m^2); and LAI is the leaf area index (m^2/m^2).

The daily crop evapotranspiration (ET_c) was calculated following the water balance method [24,40].

$$ET_c = I + P - D - R - \sum_{i=1}^n (\Delta\theta) \times \Delta Z_i \quad (4)$$

where I is irrigation amount (mm); P is the effective rainfall (mm); D is the deep percolation (mm); R is runoff; n is soil layers number; $\Delta\theta$ is the volumetric SWC stored at soil profile ($\text{cm}^3 \text{ cm}^{-3}$); ΔZ is each soil layer thickness (mm). The experiment was carried out in a greenhouse; hence, $P = 0$. As the treatments were drip irrigated and the single irrigation amount was small, $D = 0$, $R = 0$. The daily E_s was determined by subtracting T_r from ET_c .

2.3. The Modified Dual Kc Model

2.3.1. Reference Evapotranspiration

Due to the low wind speed of the greenhouse, reference evapotranspiration, ET_o , was determined by the modified Penman–Monteith method [11,41]:

$$ET_o(P - M) = \frac{0.408\Delta(R_n - G) + \gamma \frac{628}{T_a + 273}(e_s - e_a)}{\Delta + 1.24\gamma} \quad (5)$$

where ET_o is the reference crop evapotranspiration (mm.d^{-1}); R_n is net radiation ($\text{MJ.m}^{-2}.\text{d}^{-1}$); G is soil heat flux ($\text{MJ.m}^{-2}.\text{d}^{-1}$); γ is psychrometric constant ($\text{kPa. } ^\circ\text{C}^{-1}$); Δ is slope of vapor pressure curve ($\text{kPa. } ^\circ\text{C}^{-1}$); T_a is mean daily air temperature at 2 m height ($^\circ\text{C}$); e_s is the saturated vapor pressure (kPa); e_a is the actual vapor pressure (kPa).

2.3.2. Base Crop Coefficient

To accurately estimate daily T_r of the tomato, a canopy cover coefficient (K_{cc}) is introduced to obtain dynamic daily K_{cb} combining the influence of plant temperature constraint (f_t) and leaf senescence factor (f_s) [22,25].

$$K_{cb} = (1 - f_s) \left[K_{cb,\min} + K_{cc} (f_t K_{cb,\text{full}} - K_{cb,\min}) \right] \quad (6)$$

where $K_{cb,\min}$ is the minimum value of basal crop coefficient for bare soil (=0.1) [21]; $K_{cb,\text{full}}$ is the basal crop coefficient when the crop is almost completely covered by the ground, which can be expressed as follows [5,21]:

$$K_{cb,\text{full}} = \min(1.0 + 0.1h, 1.2) + [0.04(u - 2) - 0.004(RH_{\min} - 45)](h/3)^{0.3} \quad (7)$$

where h is tomato height (m); u is the wind speed at 2 m above the ground (m s^{-1}); RH_{\min} is the minimum relative humidity (%). The plant temperature constraint (f_t) is the deviation of air temperature from optimum for the crops used. The f_t is expressed as follows [5]:

$$f_t = \exp\left(-\left(\frac{T_a - T_{opt}}{T_{opt}}\right)^2\right) \quad (8)$$

where T_{opt} is the optimum air temperature (T_a) for crop growth ($^\circ\text{C}$); 26°C for greenhouse tomatoes [7,27]. The f_s is expressed as [42]:

$$f_s = 0.05 \exp\left(\frac{CDC}{0.98}t - 1\right) \quad (9)$$

where CDC is canopy decline coefficient, and 0.8 is the value recommended by Gong et al. [11]; t is the time since the beginning of canopy senescence in the late season. The K_{cc} can be calculated by using the following equation [25]:

$$K_{cc} = 1 - \exp(-k \cdot \text{LAI}) \quad (10)$$

where k is canopy extinction coefficient for solar radiation, with a value of 0.7 used in this study [17]; LAI is the leaf area index.

2.3.3. The Soil Evaporation Coefficient

Soil evaporation coefficient ($K_{e,o}$) is determined by soil surface available energy and soil water content, which is calculated according to Allen et al. [21] as:

$$K_{e,o} = K_r(K_{c,max} - K_{cb}) \leq f_{ew}K_{c,max} \quad (11)$$

where K_r is a dimensionless evaporation reduction coefficient, $K_{c,max}$ is the maximum value of K_c following the irrigation event, and f_{ew} is the fraction of soil that is both exposed and wetted.

Drip irrigation under the mulch technique was adopted in this study. Considering the effect of plastic film mulching on soil evaporation, the fraction of ground-mulching ($f_m = 0.8$) was introduced to modify original $K_{e,o}$ [25]. K_e can be expressed as:

$$K_e = (1 - f_m)K_{e,o} \quad (12)$$

According to [21], $K_{c,max}$ in Equation (11) is calculated as:

$$K_{c,max} = \max\left\{1.2 + [0.04(u - 2) - 0.004(RH_{min} - 45)](h/3)^{0.3}\right\}, (K_{cb} + 0.05) \quad (13)$$

The K_r depends on the cumulative depth of water depleted from the topsoil, which is calculated according to Zhao et al. [18]:

$$K_r = \frac{TEW - D_{e,i-1}}{TEW - REW} = \frac{1000 \cdot (SWC - 0.5\theta_{wp}) \cdot Z_e}{TEW - REW} \quad (14)$$

where $D_{e,i-1}$ is the cumulative depth of water depleted from the soil surface layer; SWC is volumetric soil water content; REW is the readily evaporable water (mm). TEW is total evaporable water (mm) and is calculated as [21]:

$$TEW = 1000(\theta_{FC} - 0.5\theta_{WP})Z_e \quad (15)$$

where Z_e is the depth of the surface soil layer dried by evaporation (m).

In Equation (11), f_{ew} is calculated as [21]:

$$f_{ew} = \min\left(1 - f_c, \left(1 - \frac{2}{3}f_c\right)f_w\right) \quad (16)$$

where f_{ew} is the fraction of surface soil evaporation; f_c is the fraction of soil surface effectively covered by vegetation, and the dynamic f_c is calculated as [43]:

$$f_c = 1.005[1 - \exp(-0.6LAI)]^{1.2} \quad (17)$$

2.3.4. Soil Water Stress Coefficient

The soil water stress coefficient (K_s) is calculated depending on available water in the effective root zone [21].

$$K_s = \begin{cases} \frac{TAW - D_{r,i}}{TAW - RAW} = \frac{TAW - D_{r,i}}{(1-p)TAW} & D_{r,i} > RAW \\ 1 & D_{r,i} \leq RAW \end{cases} \quad (18)$$

where TAW and RAW are the total and readily available soil water content in the root zone (mm), respectively; $D_{r,i}$ is the root zone depletion at the end of day i (mm); and p is the depletion fraction at the initiation of stress (dimensionless). The TAW and $D_{r,i}$ can be expressed as follows [21]:

$$TAW = 1000(\theta_{FC} - \theta_{WP})Z_r \quad (19)$$

$$D_{r,i} = D_{r,i-1} - (P_i - RO_i) - I_i - CR_i + ET_{ci} + DP_i \tag{20}$$

where Z_r is the rooting depth (m); $D_{r,i-1}$ is the root zone depletion (mm) at the end of day $i - 1$; P_i , I_i , and RO_i are the rainfall, irrigation depth, and surface runoff on day i , respectively (mm); CR_i is capillary rise from groundwater table on day i (mm); DP_i is deep percolation loss from the bottom of the root zone on day i (mm).

2.3.5. Calibration and Validation of Parameters

The parameters of the modified dual K_c method were calibrated using measured data under different irrigation treatments in 2020 and then validated by the corresponding data of 2021. The parameters required for the modified model are presented in Table 2.

Table 2. Parameters of the modified dual crop coefficient model for the greenhouse tomatoes.

Parameters	Values	Source
P_{ini}	0.50	Calibrated
P_{dev}	0.50	Calibrated
P_{mid}	0.50	Calibrated
P_{end}	0.50	Calibrated
REW (mm)	8	Calibrated
TEW (mm)	28	Calibrated
Z_e (mm)	0.10	Allen et al. [21]
Z_r	0.2/1.0	Measured

Note: p , evapotranspiration depletion fraction during the initial (P_{ini}), development (P_{dev}), middle (P_{mid}), and late (P_{end}) stages; TEW, total evaporable water; REW, readily evaporable water; Z_e , depth of the soil evaporation layer; Z_r , root depth.

2.4. Statistical Analysis

In this study, the statistical indicators, including determinant coefficient (R^2), root mean square error (RMSE), mean absolute error (MAE), modeling efficiency (EF) and index of agreement (d_{IA}), were performed to assess the modified model performance and are described as follows:

$$R^2 = \left[\frac{\sum_{i=1}^n (O_i - \bar{O})(P_i - \bar{P})}{\sqrt{\sum_{i=1}^n (O_i - \bar{O})^2} \sqrt{\sum_{i=1}^n (P_i - \bar{P})^2}} \right]^2 \tag{21}$$

$$RMSE = \left[\frac{\sum_{i=1}^n (O_i - P_i)^2}{n} \right]^{0.5} \tag{22}$$

$$MAE = \frac{1}{n} \sum_{i=1}^n |O_i - P_i| \tag{23}$$

$$EF = 1.0 - \frac{\sum_{i=1}^n (O_i - P_i)^2}{\sum_{i=1}^n (O_i - \bar{O})^2} \tag{24}$$

$$d_{IA} = 1.0 - \frac{\sum_{i=1}^n (O_i - P_i)^2}{\sum_{i=1}^n (|P_i - \bar{O}| + |O_i - \bar{O}|)^2} \tag{25}$$

where P_i and O_i are the simulated and measured values, respectively, \bar{P} and \bar{O} represent the mean simulated and measured values, and n is number of observations.

Path analysis can elucidate the direct and indirect effects from independent to dependent variables and the independent variables with multi-collinearity to explain the degree of effects of all factors [12]. A detailed description can be found in the references [5,11]. The path analysis method was employed in this study to further explore the main controlling factors of daily ET_c and its components with environmental (R_n , T_a , VPD, SWC, and u) and biophysical factors (K_{cc}) under different irrigation conditions.

3. Results

3.1. Microclimate Conditions in the Greenhouse

Variations of daily meteorological factors inside the greenhouse during tomato growth states in 2020 and 2021 are shown in Figure 4. In general, there were similar microclimate conditions in the greenhouse for the two years. The RH remained relatively high as a result of the semi-closed environment of the greenhouse. The values of daily average RH were 76.50% and 74.94%, and the highest values in the two seasons are 97.38% and 94.37%, respectively. VPD showed an opposite trend compared with RH . The daily average VPD varied from 0.03 to 2.68 kPa in 2020 and from 0.06 to 2.41 kPa in 2021. The daily air temperature (T_a) ranged from 8.73 to 27.52 and 9.84 to 28.73 °C, with mean values of 20.09 and 19.41 °C in the two seasons, respectively. The average values of u were 0.063 and 0.059 $m\ s^{-1}$ during experimental periods in the two years, respectively. The R_n showed a similar trend with ET_o . The average values of R_n were 4.88 and 4.32 $MJ\ m^{-2}\ d^{-1}$, while ET_o were 1.88 and 1.96 mm in 2020 and 2021, respectively. The total seasonal ET_o values were 229.0 and 235.3 $mm\cdot d^{-1}$, respectively, during the whole growing period in two years.

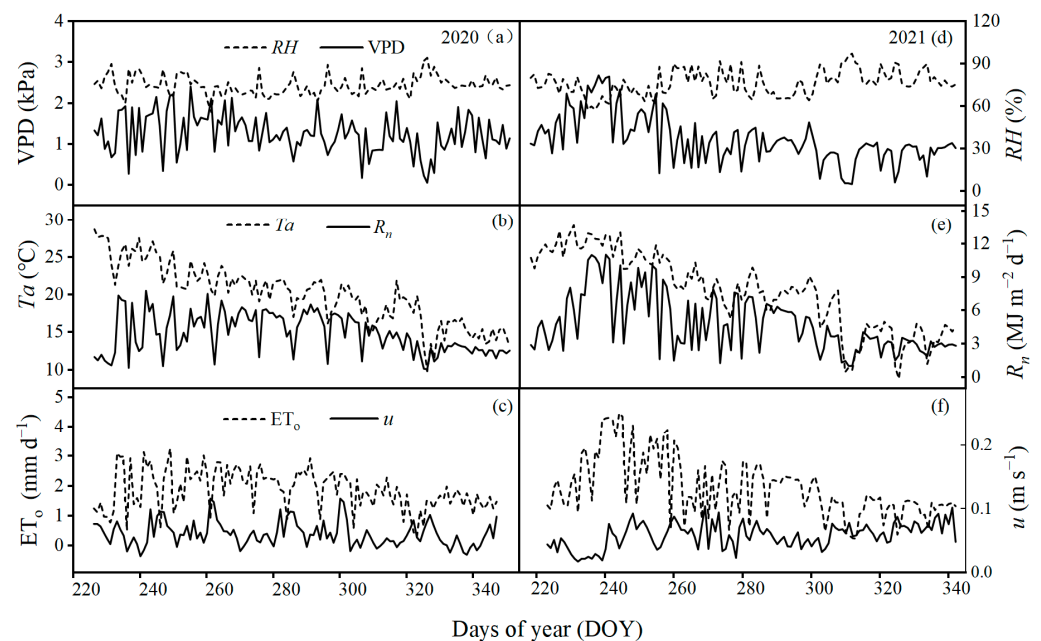


Figure 4. The meteorological conditions, i.e., vapor pressure deficit (VPD), relative humidity (RH), air temperature (T_a), net radiation (R_n), wind speed (u), and reference in the 2020 (a–c) and 2021 (d–f).

3.2. Basal Crop, Plant Temperature Constraint, Soil Evaporation, and Water Stress Coefficients Dynamics

As Figure 5a,d shows, the values of K_{cb} were similar among treatments during the initial stage when all treatments were fully irrigated and started to separate during the development stage when differential irrigations were performed. During the middle stage, the K_{cb} reached the maximum value when the plant canopy fully developed and, thereafter, began to decline until the end of the season. The values of K_{cb} showed day-to-day fluctuation ranging from 0.11–0.33, 0.30–0.96, 0.70–1.09, and 0.53–1.03 for the initial,

development, middle, and late plant growth stages, respectively. Notably, the late season K_{cb} values fluctuated greatly, especially after about day of year (DOY) 300 in 2021, mainly attributed to K_{cb} varying widely with climatic conditions. Moreover, the K_{cb} increased with the improvement in irrigation level, and the average value of K_{cb} over 2020 to 2021 under the W3 treatment was 0.73, which increased by 6.90% and 8.35% compared with those of W2 and W3 treatments, respectively.

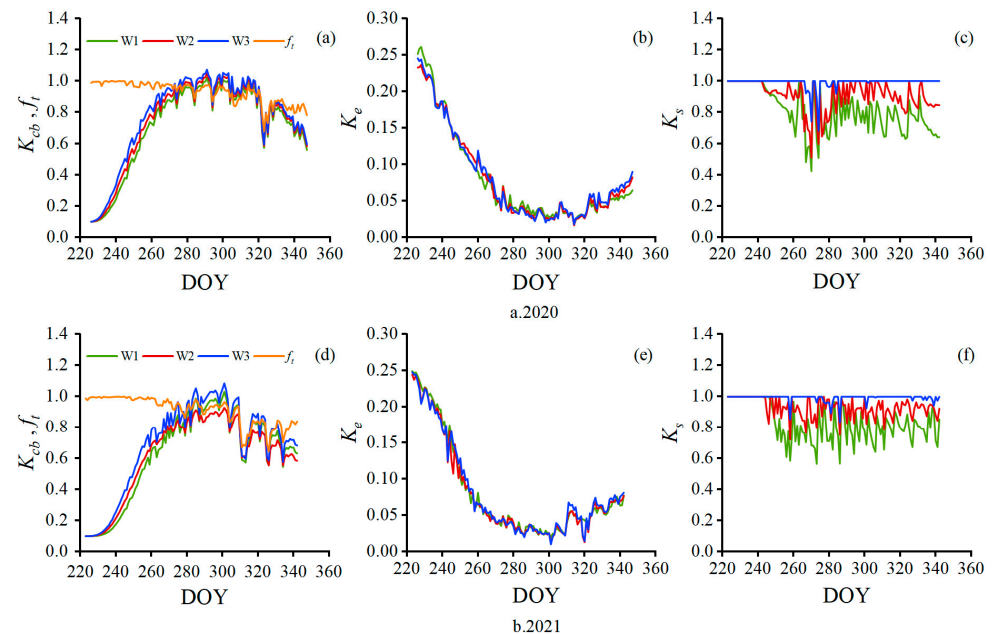


Figure 5. The variations of basal crop coefficient (K_{cb}), soil evaporation coefficient (K_e), and soil water stress coefficient (K_s) for different irrigation treatments and plant temperature constraint (f_t) in the 2020 (a–c) and 2021 (d–f).

The f_t was high and fluctuated slightly because the T_a was close to the T_{opt} during the initial stage of the greenhouse tomato (Figure 5a,d). As the temperature decreased, T_a deviated significantly from the T_{opt} (Figure 5b,e), resulting in low values of f_t and large variation during the middle and late stages. Additionally, the f_t had little influence on K_{cb} at the initial stage because the fraction of canopy cover was quite small. With the increase in LAI, the variation of K_{cb} was closely correlated with the dynamics of f_t (Figure 5a,d, Equation (6)), which is similar to the results from Qiu et al. [15]. Thus, these results can provide a basis for considering f_t in the modified dual K_c model to estimate ET_c during the whole growing season of greenhouse-grown tomatoes.

The K_e values of different irrigation treatments were almost the same (Figure 5b,e). At the initial stage, the K_e was high due to the small canopy coverage and more soil surface exposed area, reaching its maximum value of 0.26 in two study years. After tomato plants grew rapidly, the K_e values showed a significant decreasing trend from the initial to the beginning of the middle stage. In the middle stage, the K_e appeared to remain constant and was less than 0.05, which implied that almost no soil evaporation occurred in this stage. At the late plant growth stage, it showed a small upward trend because the canopy cover decreased due to leaf senescence. The variation of K_e was highly linked to the topsoil moisture dictated by the occurrence of irrigation; K_e increased after irrigation and then gradually declined with the drying of the soil.

Figure 5c,f illustrated that the K_s value was 1.0 during the initial stage in both years, indicating that the tomato growth did not experience soil water depletion. However, after the tomato's initial stage, the variations of W1, W2, and W3 treatments showed obvious differences. The K_s value under W3 treatment suggested that minor water stress occurred for a few days during the tomato's whole growth period in 2020 and 2021, while for W1 and W2 treatments, the plants were under soil water stress conditions starting with the

plant development stage until the end season, with the K_s curve showing a periodical variation due to irrigation. Furthermore, the K_s value of W2 treatment remained above 0.72, except for 270–280 DOY in 2020. The W1 treatment also did not fall below 0.42, and the average K_s values of W1 and W2 treatments were 0.82 and 0.92, respectively, during the two growing seasons. These results demonstrated that the water stress degree of different irrigation treatments was $W1 > W2 > W3$.

3.3. Assessing the Modified Dual Crop Coefficient Mode

Comparison and correlation of ET_c and its components of greenhouse tomatoes between measurements and estimations under different irrigation treatments in 2020 and 2021 are presented in Figure 6 and Table 3. Results showed that the simulated results were well in agreement with the measured ones over both years (Table 3). The b_0 and R^2 for comparison of simulated T_r with measured values ranged from 0.84 to 1.04 and from 0.95 to 0.98 over both years. The residual estimation errors were small, with the MAE values varying from 0.18 to 0.26 mmd^{-1} and the RMSE from 0.21 to 0.33 mmd^{-1} . Also, the EF and d_{IA} values resulted in relatively high values ranging from 0.76 to 0.85 and 0.91 to 0.95, respectively. Similarly, good agreements were found between the measured and simulated daily ET_c for three irrigation treatments in two study years. The b_0 values were higher than 0.86, and the R^2 ranged from 0.89 to 0.95 among treatments. The MAE and RMSE varied from 0.29 to 0.41 and from 0.36 to 0.51 mm d^{-1} , respectively. The EF varied from 0.75 to 0.81, and the d_{IA} of all treatments was above 0.90. In addition, the modified dual K_c model could estimate E_s reasonably, with b_0 of 0.81–0.97, R^2 of 0.89–0.93, MAE of 0.03–0.04 mm d^{-1} , RMSE of 0.03–0.04 mm d^{-1} , EF of 0.71–0.78, and d_{IA} of 0.92–0.94, respectively. Overall, these indicators show that the modified dual K_c model has high simulation accuracy for ET_c and its components of greenhouse-grown tomatoes with drip irrigation under mulch in Northeast China.

Table 3. Statistical results of the measured and simulated daily evapotranspiration and its component using the modified dual K_c model on greenhouse tomatoes under different irrigation treatments in 2020 and 2021.

Variable	Treatments	Year	b	R^2	MAE (mm/d)	RMSE (mm/d)	EF	d_{IA}
T_r	W1	2020	0.88	0.97	0.25	0.33	0.77	0.93
		2021	0.84	0.95	0.23	0.27	0.76	0.91
	W2	2020	0.90	0.98	0.22	0.26	0.81	0.95
		2021	0.88	0.98	0.26	0.29	0.80	0.93
	W3	2020	1.04	0.97	0.18	0.21	0.83	0.95
		2021	0.95	0.95	0.19	0.28	0.85	0.91
ET_c	W1	2020	0.86	0.89	0.39	0.48	0.75	0.92
		2021	0.89	0.94	0.29	0.36	0.80	0.92
	W2	2020	0.92	0.93	0.35	0.40	0.79	0.90
		2021	1.09	0.88	0.41	0.51	0.78	0.91
	W3	2020	0.88	0.95	0.35	0.41	0.76	0.90
		2021	1.01	0.89	0.37	0.43	0.81	0.92
E_s	W1	2020	0.86	0.92	0.03	0.04	0.74	0.92
		2021	0.90	0.92	0.03	0.03	0.78	0.94
	W2	2020	0.81	0.91	0.04	0.04	0.73	0.92
		2021	0.97	0.89	0.03	0.04	0.71	0.92
	W3	2020	0.92	0.89	0.04	0.04	0.75	0.93
		2021	0.86	0.93	0.03	0.04	0.76	0.93

Note: b is slope of the least square regression line; R^2 is coefficients of determination; MAE is mean absolute error (mm d^{-1}); RMSE is root mean square error (mm d^{-1}); EF is the modeling efficiency; d_{IA} is index of agreement.

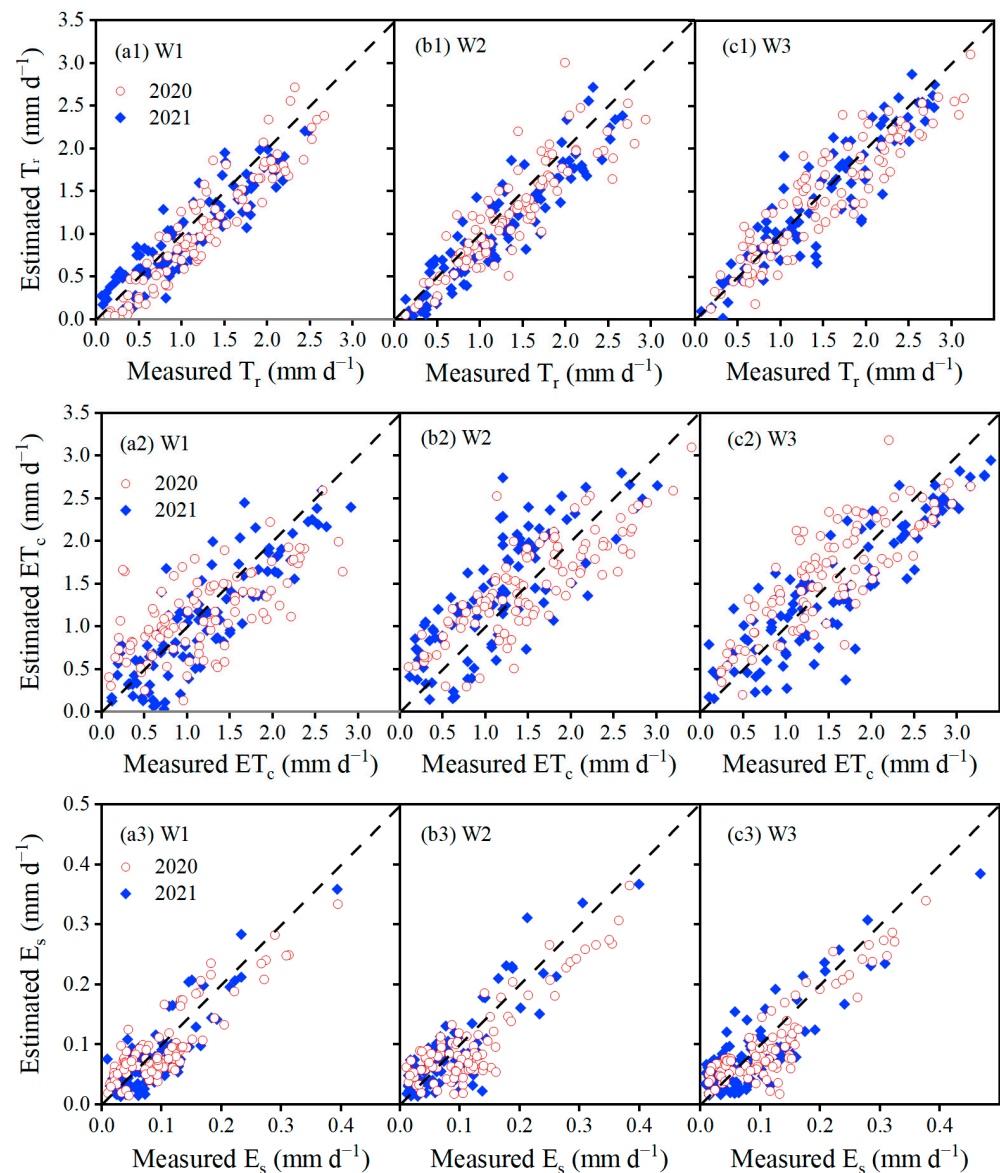


Figure 6. Comparison of daily measured and estimated values of evapotranspiration (ET_c) (a1–c1), tomato plant transpiration (T_r) (a2–c2), and soil evaporation (E_s) (a3–c3) under different irrigation treatments in 2020 and 2021.

3.4. Crop Evapotranspiration Partitioning in Different Growth Stages

The seasonal variations of simulated T_r , E_s , and ET_c showed similar patterns under different irrigation treatments over both years (Figure 7). The daily T_r of greenhouse tomatoes gradually increased during the initial stage, peaked at the plant middle stage (2.67 – 3.15 mm d^{-1}), and subsequently decreased at the late stage. The daily values of E_s were high, with the maximum daily E_s of 0.67 – 0.73 mm d^{-1} at the initial stage. As the fraction of canopy coverage increased, the E_s values started to rapidly decrease and then approached zero. The daily ET_c of tomatoes varied with changes in T_r and E_s , which were mainly affected by soil evaporation at the initial stage and by plant transpiration at the development, middle, and late stages. In addition, higher irrigation amounts resulted in higher T_r and ET_c during the plant growth season. The daily average values of T_r and ET_c in both years under the W3 treatment increased by 38.4% and 32.9%, respectively, compared to those under the W1 treatment.

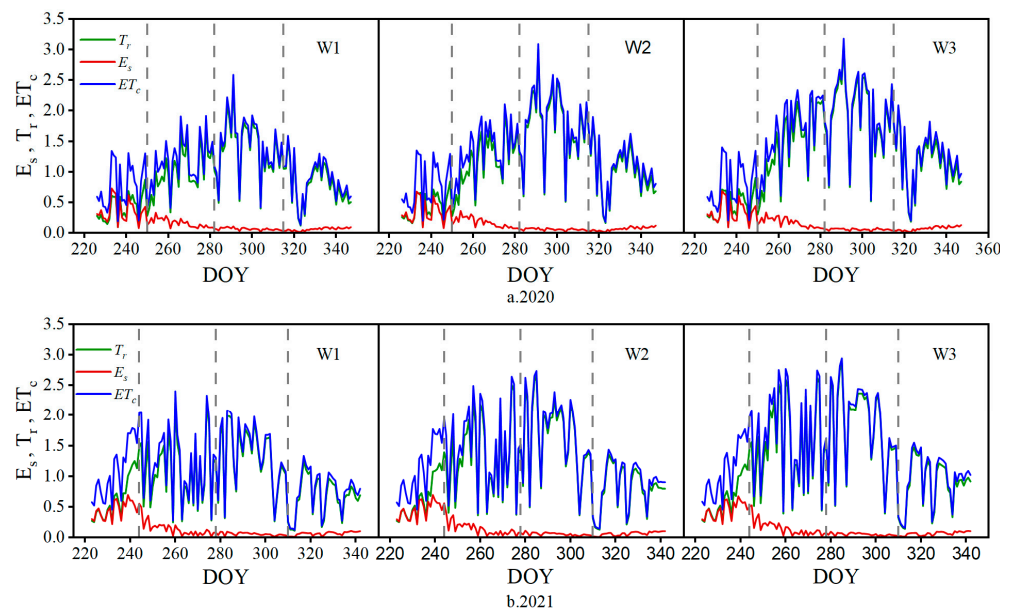


Figure 7. Seasonal variations in evapotranspiration (ET_c), evaporation (E_s), and transpiration (T_r) of greenhouse tomatoes for different treatments during the growing season in 2020 and 2021.

The simulated crop evapotranspiration and its components under different irrigation treatments at different growth stages in 2020 and 2021 are shown in Table 4. The results indicate that T_r ranged from 12.3–14.5 mm and E_s ranged from 8.6–11.8 mm at the initial plant growth stage. The highest E_s/ET_c (38.3–44.9%) at this stage resulted from the small LAI and high soil moisture at the topsoil layer. In the development plant growth stage, T_r gradually increased, and then E_s significantly decreased with the increase in canopy coverage. The T_r , E_s , and E_s/ET_c values were 36.4–62.1 mm, 5.2–6.6 mm, and 8.1–14.7% in the two years, respectively. In the middle plant growth stage, T_r reached the maximum (43.4–65.0 mm), but E_s was at its minimum (1.7–2.0 mm). Meanwhile, E_s/ET_c decreased to the lowest level ranging from 2.8–4.3%. In the late plant growth stage, T_r and E_s were relatively low due to leaf senescence of tomatoes and lower solar radiation and temperature. For the whole growth stages, the T_r , E_s , ET_c , and E_s/ET_c values were 116.5–175.9 mm, 18.3–21.9 mm, 138.5–194.4 mm, and 9.5–15.8% from 2020 to 2021, respectively. It also can be seen from Table 4 that E_s showed no obvious differences among the three treatments at different growth stages. T_r and ET_c in tomato growth stages, except for its initial stage, increased with the increase in irrigation amount, but the opposite trend was observed for E_s/ET_c .

Table 4. Transpiration (T_r), soil evaporation (E_s), evapotranspiration (ET_c), and ratio of evaporation and transpiration to evapotranspiration for the three treatments (W1–W3) at different growth stages of greenhouse tomatoes in 2020 and 2021.

Growth Stage	Years	T_r (mm)			E_s (mm)			ET_c (mm)			E_s/ET_c (%)		
		W1	W2	W3	W1	W2	W3	W1	W2	W3	W1	W2	W3
Initial	2020	12.3	13.9	12.8	8.8	8.6	8.6	21.1	22.5	21.4	41.8	38.3	40.2
	2021	14.5	14.3	14.4	11.8	11.3	11.2	26.3	25.6	26.0	44.9	44.2	43.1
Development	2020	43.7	50.9	62.1	5.2	5.5	5.5	48.9	56.4	67.6	10.7	9.7	8.1
	2021	36.4	46.9	55.3	6.3	6.1	6.6	42.6	53.0	61.9	14.7	11.6	10.7
Middle	2020	48.7	59.7	65.0	2.2	2.0	2.0	50.9	61.7	67.0	4.3	3.3	2.9
	2021	43.4	52.4	57.6	1.7	1.7	1.6	45.1	54.1	59.3	3.8	3.1	2.8
Late	2020	25.3	31.1	36.0	2.1	2.2	2.5	27.4	33.4	38.5	7.5	6.7	6.4
	2021	22.3	26.3	28.9	2.1	2.0	2.2	24.4	28.4	31.1	8.6	7.2	7.0
Whole stage	2020	130.0	155.7	175.9	18.3	18.4	18.5	148.4	174.1	194.4	12.4	10.6	9.5
	2021	116.5	140.0	156.7	21.9	21.1	21.6	138.5	161.1	178.3	15.8	13.1	12.1

3.5. Path Analysis between Evapotranspiration Partitioning and Other Factors

To further explore the mechanism of environmental and biophysical factors on daily evapotranspiration and its components of greenhouse tomatoes, the path analysis results between simulated daily T_r , E_s , and ET_c and each factor (i.e., R_n , T_a , VPD, K_{cc} , SWC, and u) under different irrigation conditions during 2020–2021 are presented in Table 5. With regard to T_r , the correlation coefficient between T_r and the factors turned out to be R_n (0.580) > VPD (0.344) > SWC (−0.299) > K_{cc} (0.229) > T_a (0.134) > u (0.060). The three primary direct effect factors on T_r were R_n (0.620), K_{cc} (0.424), and T_a (0.175). The direct effects of VPD (−0.042) and u (0.018) on T_r were not significant ($P > 0.05$), but the indirect actions of VPD were high through the R_n (0.464). The effect of SWC on T_r was mainly through the indirect path of K_{cc} (−0.276) on T_r . The values of the decision coefficient showed that R_n (1.103) was the most influential decision factor affecting T_r .

Table 5. Path analysis results between estimated transpiration (T_r), soil evaporation (E_s), and evapotranspiration (ET_c) and impact factors under different irrigation treatments during two growing seasons.

Factors	b_i	$r_{ij}b_i$							r_{iy}	R_i^2	
		Σ	R_n	T_a	VPD	K_{cc}	SWC	u			
T_r	R_n	0.620 **	−0.040		0.098	−0.031	−0.104	−0.001	−0.001	0.580 **	1.103
	T_a	0.175 **	−0.041	0.348		−0.027	−0.314	−0.046	−0.002	0.134 **	0.078
	VPD	−0.042	0.386	0.464	0.112		0.052	0.045	0.001	0.344 **	−0.027
	K_{cc}	0.424 **	−0.195	−0.152	−0.130	0.017		0.066	0.004	0.229 **	0.374
	SWC	−0.101 **	−0.197	0.009	0.079	−0.007	−0.276		−0.003	−0.299 **	0.071
	u	0.018	0.042	−0.041	−0.021	0.003	0.087	0.014		0.060	0.002
	R_n	0.418 **	0.147		−0.247	0.176	0.215	0.002	0.001	0.564 **	0.647
E_s	T_a	−0.440 **	1.096	0.235		0.150	0.649	0.061	0.002	0.656 **	−0.383
	VPD	0.235 **	0.410	0.313	−0.281		0.356	0.021	0.001	0.645 **	0.358
	K_{cc}	−0.876 **	0.037	−0.103	0.326	−0.096		−0.087	0.003	−0.839 **	2.237
	SWC	0.134 **	0.416	0.006	−0.199	0.037	0.571		0.002	0.551 **	0.166
	u	−0.015	−0.188	−0.028	0.052	−0.015	−0.179	−0.019		−0.203 **	0.006
	R_n	0.673 **	−0.015		0.066	−0.004	−0.075	−0.001	−0.001	0.658 **	1.339
	T_a	0.118 *	0.111	0.378		−0.003	−0.225	−0.037	−0.002	0.228 **	0.068
ET_c	VPD	−0.005	0.441	0.503	0.075		−0.124	−0.013	−0.001	0.436 **	−0.004
	K_{cc}	0.304 **	−0.265	−0.166	−0.087	0.002		−0.013	−0.001	0.110 **	0.159
	SWC	−0.082 *	−0.132	0.010	0.053	−0.001	−0.198		0.003	−0.220 **	0.043
	u	0.017	0.016	−0.044	−0.014	−0.000	0.062	0.012		0.032	0.001
	R_n	0.673 **	−0.015		0.066	−0.004	−0.075	−0.001	−0.001	0.658 **	1.339

Note: b_i , $r_{ij}b_j$, r_{iy} , and R_i^2 are the direct path coefficient, indirect path coefficient, total correlation coefficient, and decision coefficient, respectively. Σ is the sum of the indirect path coefficients of each variable. The ** and * represent significant correlation at level 0.01 and 0.05, respectively.

In terms of the total correlation between E_s and impact factors, a higher correlation was observed in K_{cc} (−0.839), followed by T_a , VPD, R_n , SWC, and u (0.656, 0.645, 0.564, 0.551, and −0.203, respectively), where the corresponding direct path coefficients were −0.876, −0.440, 0.235, 0.418, 0.134, and −0.015, respectively. The correlation (−0.839) and the direct effect (−0.876) between E_s and K_{cc} were both the highest, and there was a significantly negative relationship. The indirect effect of T_a (1.096) on E_s was the maximum, and the influence of T_a on E_s was mainly through the indirect path of K_{cc} (0.649) and R_n (0.235). The decision coefficients indicated that the K_{cc} (2.237) was the dominant factor on E_s , followed by R_n (0.647), while T_a (−0.383) was the main environment limiting factor on E_s .

As for ET_c , higher correlations were observed in R_n , VPD, and T_a (0.658, 0.436, and 0.228, respectively), and lower correlations in SWC, K_{cc} , and u (−0.220, 0.110, and 0.032, respectively). The direct path coefficients of R_n (0.673), K_{cc} (0.304), and T_a (0.118) were greater than the corresponding total indirect path coefficients (−0.015, −0.265, and 0.111, respectively), indicating that the influence of these factors was mainly through the direct path. The indirect effect of SWC (−0.132) on ET_c was primarily through the path of K_{cc}

(−0.198). Furthermore, the decision coefficient for R_n (0.658) was the highest, indicating that R_n was the dominant factor accounting for changes in ET_c .

4. Discussion

4.1. Plant Temperature Constraint and Basal Crop Coefficients

Protected tomato cultivation is often subjected to a wide range of low-temperature stress in Northeast China during the winter season [44]. Temperatures mostly below the optimal range of 25–27 °C are required for good tomato growth in systems using unheated greenhouses [27,45], which can also be observed in Figure 4b,e. Low-temperature stress inhibits stomatal opening and induces stomatal closure, thereby leading to a decrease in plant transpiration rate [46,47]. Moreover, low temperatures may restrict water uptake and mobility in roots and xylem, which ultimately leads to canopy stomatal closure [48] and affects T_r . Transpiration is lost mainly through plant stomata [31]; therefore, in this study, the temperature constraint for stomatal conductance was taken into account in the modified dual K_c model by using the plant temperature constraint coefficient (f_t).

The base crop coefficient (K_{cb}) was influenced by crop types, climate, soil surface mulching, irrigation method, and other management factors [3]. The highest average values of K_{cb} were 0.99 and 0.96 observed from W3 treatment at the middle stage in 2020 and 2021, respectively (Figure 5a,d), which were lower than the standard value (1.10) proposed by FAO 56. The results are consistent with previous studies [15,49,50], and the possible reasons for this are as follows: (1) higher humidity and lower wind speed in the greenhouse environment could lead to lower K_{cb} values [22]; (2) the effects of the plant temperature constraints and leaf senescence on T_r were considered in our study, which decreased the K_{cb} ; (3) using plastic mulch may decrease the FAO tabulated K_{cb} values by 10–30% [21].

Figure 8 shows the relationship between the LAI and K_{cb} for greenhouse tomatoes over the whole growth period in 2020 and 2021. LAI is an important physiological index used to characterize plant canopy development and is highly linked to the variability in plant transpiration [49]. In this study, a significant logarithmic relationship was found between LAI and K_{cb} with R^2 values of 0.97 and 0.80, respectively. The K_{cb} value sharply increased with increased LAI when $LAI < 2 \text{ m}^2 \text{ m}^{-2}$ and increased slowly when $LAI > 2 \text{ m}^2 \text{ m}^{-2}$. The K_{cb} change rate started to slow down beyond the threshold LAI, which could be attributed to crop canopy being gradually saturated, and the increase rate of energy intercepted by the canopy was relatively low [21,51,52]. In addition, at the late plant growth stage, the leaf senescence and reduction of physiological activity could induce stomatal closure, significantly affecting the plant transpiration and, hence, the K_{cb} change rate [25,42].

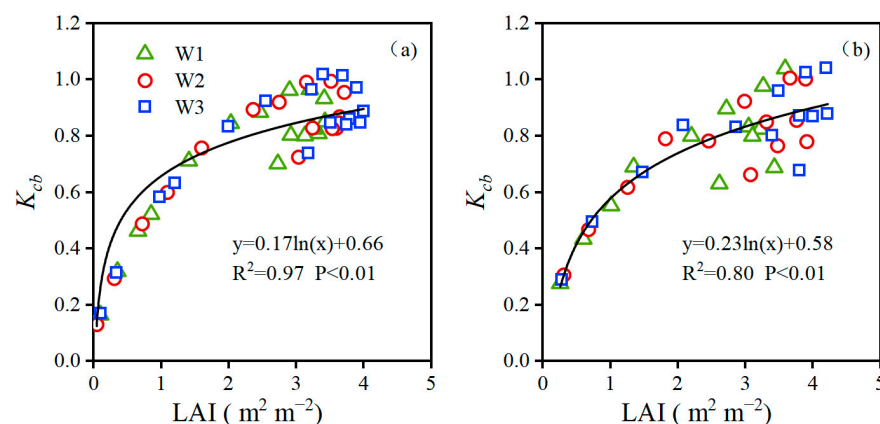


Figure 8. Relationship between leaf area index (LAI) and basal crop coefficient (K_{cb}) during the growing seasons of tomato in 2020 (a) and 2021 (b) under different irrigation treatments.

4.2. Characteristics of Tomato Evapotranspiration Partitioning

Plastic mulch and drip irrigation would affect the energy exchange between the soil and the atmosphere, which could effectively reduce soil evaporation and, thus, enhance water use efficiency [35,49]. The values of E_s/ET_c in this study varied from 9.5% to 15.8%, indicating that T_r was the dominant portion of ET_c during the growing period in the two years. The obtained E_s/ET_c values were lower than the result of Gong et al. [53], which ranged from 24–26% for greenhouse tomatoes under drip irrigation without film mulching. Furthermore, in our experimental treatments, the cumulative values of soil evaporation were quite small and showed no apparent differences between the different treatments, ranging from 18.3 to 21.9 mm over the whole growing season in the two years. This result may be related to the use of drip irrigation under mulch technology for greenhouse tomatoes in the present study. In this irrigation system, the area of irrigated wetness and bare soil were small [54]. Although reduced irrigation did decrease the canopy cover and increase the soil surface exposed area, the actual wet soil evaporation area did not increase, so there were no obvious differences in E_s among the treatments.

The total ET_c values of greenhouse tomatoes over the whole growth period in our study (138.5–194.4 mm) were comparable with the values (147–225 mm) reported by Mukherjee et al. [55] in India but generally less than those reported by Gong et al. [7] in the North China Plain (315.1–350.8 mm) and by Hanson and May (2005) in San Joaquin Valley, California, USA (528–752 mm). The lower cumulative ET_c of this study may have resulted from the differences in adopted management practices, crop cultivars, growing seasons, soil characterization, and climate conditions of the study region [5,56,57]. In addition, irrigation level has an important influence on the variations of evapotranspiration, especially in a greenhouse [11]. Several studies indicated that ET_c under a high irrigation amount is typically greater than that under a low irrigation amount [28,58–60]. The results of the present study showed that the seasonal total ET_c values in both years under the W3 treatment were 11.4% and 31.1% higher than under the W2 and W1 treatments, respectively. This result could be attributed to the differences in soil water content between the soil body and root cell, resulting in a water potential gradient. A higher soil water potential gradient can effectively promote water migration in the soil–plant–atmosphere [28].

4.3. Main Controlling Factors on Evapotranspiration and Its Components

Previous studies indicated that meteorological conditions (e.g., solar radiation, air temperature, relative humidity, vapor pressure deficit, and wind speed) were the main influencing factors on ET_c [5,12], and soil water content and canopy characteristics also have an important influence on T_r [61]. Path analysis results in this study showed that R_n was the main meteorological controlling factor affecting the variations of daily ET_c and T_r , which were in agreement with the results of Alberto et al. [62]. This is mainly because solar radiation not only induces the opening and closing of leaf stomata but also causes the variation of T_a and RH [5]. Also, R_n could cause the leaf surface temperature to increase VPD between the inside of the leaf and the outside air, thus promoting T_r and ET_c [11]. Additionally, our results showed that a significant negative correlation existed between E_s and K_{cc} , while a significant positive correlation existed between E_s and T_a . Similar results have been found by Zheng et al. [31] for rainfed maize in Northern China. The possible reason is that more energy reached the soil surface when canopy coverage was small and increased the soil temperature, resulting in an increase in E_s .

5. Conclusions

In this study, the modified dual K_c model, considering the effects of plant temperature constraints (f_t) and leaf senescence (f_s) on T_r and the effects of ground-mulching (f_m) and soil moisture content (SWC) on E_s , was evaluated for estimating ET_c of greenhouse tomatoes under different irrigation conditions. The goodness of fit indicators showed that the modified dual K_c model performed well in estimating ET_c and its components. The results indicated that the seasonal total T_r , E_s , and ET_c for W1–W3 treatments were

116.5–175.9 mm, 18.3–21.9 mm, and 138.5–194.4 mm, respectively, and that E_s/ET_c was 9.5%–15.8% over the two growing seasons. In addition, T_r and ET_c of greenhouse tomatoes illustrated an increasing trend with the increase in irrigation amount, whereas E_s/ET_c followed the opposite trend. The path analysis results showed that R_n was the main meteorological factor controlling T_r and ET_c , K_{cc} was the dominant controlling factor affecting E_s , followed by R_n , while T_a was the primary limiting factor affecting E_s . The results of this study provide a theoretical basis for forming effective irrigation scheduling and improving water resources management in Northeast China.

Author Contributions: Conceptualization, M.Y. and B.L.; methodology, J.W. and M.G.; software, Z.X. and T.W.; validation, M.G., L.S. and D.N.; formal analysis, M.Z. and H.N.; investigation, M.G., L.S. and D.N.; resources, T.W. and J.W.; data curation, M.Y., M.Z. and H.N.; writing—original draft preparation, M.G.; writing—review and editing, M.Y., B.L., L.M. and J.W.; visualization, M.Y. and M.G.; supervision, M.Y., B.L. and L.M.; project administration, T.W. and J.W.; funding acquisition, M.Y. All authors have read and agreed to the published version of the manuscript.

Funding: This study was funded by the China Postdoctoral Science Foundation (2019M661128).

Institutional Review Board Statement: Not applicable.

Data Availability Statement: Not applicable.

Acknowledgments: We acknowledge the staff of Shenyang Agricultural University for their technical support.

Conflicts of Interest: The authors declare no conflict of interest.

References

- Gorjian, S.; Calise, F.; Kant, K.; Ahamed, M.S.; Copertaro, B.; Najafi, G.; Zhang, X.; Aghaei, M.; Shamshiri, R.R. A review on opportunities for implementation of solar energy technologies in agricultural greenhouses. *J. Clean. Prod.* **2021**, *285*, 124807. [\[CrossRef\]](#)
- Li, B.; Wim, V.; Shukla, M.K.; Du, T. Drip irrigation provides a trade-off between yield and nutritional quality of tomato in the solar greenhouse. *Agric. Water Manag.* **2021**, *249*, 106777. [\[CrossRef\]](#)
- Libardi, L.G.P.; de Faria, R.T.; Dalri, A.B.; Rolim, G.D.; Palaretti, L.F.; Coelho, A.P.; Martins, I.P. Evapotranspiration and crop coefficient (kc) of pre-sprouted sugarcane plantlets for greenhouse irrigation management. *Agric. Water Manag.* **2019**, *212*, 306–316. [\[CrossRef\]](#)
- Contreras, J.I.; Alonso, F.; Canovas, G.; Baeza, R. Irrigation management of greenhouse zucchini with different soil matric potential level. Agronomic and environmental effects. *Agric. Water Manag.* **2017**, *183*, 26–34. [\[CrossRef\]](#)
- Qiu, R.J.; Liu, C.W.; Cui, N.B.; Wu, Y.J.; Wang, Z.C.; Li, G. Evapotranspiration estimation using a modified priestley-taylor model in a rice-wheat rotation system. *Agric. Water Manag.* **2019**, *224*, 105755. [\[CrossRef\]](#)
- Katsoulas, N.; Stanghellini, C. Modelling crop transpiration in greenhouses: Different models for different applications. *Agronomy* **2019**, *9*, 392. [\[CrossRef\]](#)
- Gong, X.W.; Qiu, R.J.; Ge, J.K.; Bo, G.K.; Ping, Y.L.; Xin, Q.S.; Wang, S.S. Evapotranspiration partitioning of greenhouse grown tomato using a modified priestley-taylor model. *Agric. Water Manag.* **2021**, *247*, 106709. [\[CrossRef\]](#)
- Huang, S.; Yan, H.F.; Zhang, C.; Wang, G.Q.; Acquah, S.J.; Yu, J.J.; Li, L.L.; Ma, J.M.; Darko, R.O. Modeling evapotranspiration for cucumber plants based on the shuttleworth-wallace model in a venlo-type greenhouse. *Agric. Water Manag.* **2020**, *228*, 105861. [\[CrossRef\]](#)
- Zhao, P.; Li, S.; Li, F.; Du, T.; Tong, L.; Kang, S. Comparison of dual crop coefficient method and shuttleworth-wallace model in evapotranspiration partitioning in a vineyard of northwest china. *Agric. Water Manag.* **2015**, *160*, 41–56. [\[CrossRef\]](#)
- Pereira, L.S.; Paredes, P.; Jovanovic, N. Soil water balance models for determining crop water and irrigation requirements and irrigation scheduling focusing on the fao56 method and the dual kc approach. *Agric. Water Manag.* **2020**, *241*, 106357. [\[CrossRef\]](#)
- Gong, X.W.; Qiu, R.J.; Sun, J.S.; Ge, J.K.; Li, Y.B.; Wang, S.S. Evapotranspiration and crop coefficient of tomato grown in a solar greenhouse under full and deficit irrigation. *Agric. Water Manag.* **2020**, *235*, 106154. [\[CrossRef\]](#)
- Zhang, B.Z.; Xu, D.; Liu, Y.; Li, F.S.; Cai, J.B.; Du, L.J. Multi-scale evapotranspiration of summer maize and the controlling meteorological factors in north china. *Agric. For. Meteorol.* **2016**, *216*, 1–12. [\[CrossRef\]](#)
- Allen, R.G.; Pruitt, W.O.; Wright, J.L.; Howell, T.A.; Ventura, F.; Snyder, R.; Itenfisu, D.; Steduto, P.; Berengena, J.; Yrisarry, J.B.; et al. A recommendation on standardized surface resistance for hourly calculation of reference eto by the fao56 penman-monteith method. *Agric. Water Manag.* **2006**, *81*, 1–22. [\[CrossRef\]](#)
- Shuttleworth, W.J.; Wallace, J. Evaporation from sparse crops-an energy combination theory. *Q. J. R. Meteorol. Soc.* **1985**, *111*, 839–855. [\[CrossRef\]](#)

15. Qiu, R.J.; Li, L.G.; Liu, C.W.; Wang, Z.; Zhang, B.; Liu, Z. Evapotranspiration estimation using a modified crop coefficient model in a rotated rice-winter wheat system. *Agric. Water Manag.* **2022**, *264*, 107501. [[CrossRef](#)]
16. Wang, P.; Li, S.; Chen, Q.; Li, X.-Y.; Liu, S.; Wu, X.; Yang, X.; Xu, Z. A novel method for simulating the dynamics of the single and dual maize crop coefficients in an arid ecosystem. *Eur. J. Agron.* **2023**, *142*, 126688. [[CrossRef](#)]
17. Jiang, X.L.; Kang, S.Z.; Tong, L.; Li, S.E.; Ding, R.S.; Du, T.S. Modeling evapotranspiration and its components of maize for seed production in an arid region of northwest china using a dual crop coefficient and multisource models. *Agric. Water Manag.* **2019**, *222*, 105–117. [[CrossRef](#)]
18. Zhao, P.; Kang, S.; Li, S.; Ding, R.; Tong, L.; Du, T. Seasonal variations in vineyard et partitioning and dual crop coefficients correlate with canopy development and surface soil moisture. *Agric. Water Manag.* **2018**, *197*, 19–33. [[CrossRef](#)]
19. Zhang, B.; Liu, Y.; Xu, D.; Zhao, N.; Lei, B.; Rosa, R.D.; Paredes, P.; Paço, T.A.; Pereira, L.S. The dual crop coefficient approach to estimate and partitioning evapotranspiration of the winter wheat–summer maize crop sequence in north china plain. *Irrig. Sci.* **2013**, *31*, 1303–1316. [[CrossRef](#)]
20. Pereira, L.S.; Paredes, P.; López-Urrea, R.; Hunsaker, D.J.; Mota, M.; Mohammadi Shad, Z. Standard single and basal crop coefficients for vegetable crops, an update of fao56 crop water requirements approach. *Agric. Water Manag.* **2021**, *243*, 106196. [[CrossRef](#)]
21. Allen, R.G.; Pereira, L.S.; Raes, D.; Smith, M. Crop evapotranspiration-guidelines for computing crop water requirements-fao irrigation and drainage paper 56. *FAO Rome* **1998**, *300*, D05109.
22. Gong, X.; Liu, H.; Sun, J.; Gao, Y.; Zhang, H. Comparison of shuttleworth-wallace model and dual crop coefficient method for estimating evapotranspiration of tomato cultivated in a solar greenhouse. *Agric. Water Manag.* **2019**, *217*, 141–153. [[CrossRef](#)]
23. Yan, H.; Huang, S.; Zhang, J.; Zhang, C.; Wang, G.; Li, L.; Zhao, S.; Li, M.; Zhao, B. Comparison of shuttleworth-wallace and dual crop coefficient method for estimating evapotranspiration of a tea field in southeast china. *Agriculture* **2022**, *12*, 1392. [[CrossRef](#)]
24. Zhang, Y.; Han, W.; Zhang, H.; Niu, X.; Shao, G. Evaluating maize evapotranspiration using high-resolution uav-based imagery and fao-56 dual crop coefficient approach. *Agric. Water Manag.* **2023**, *275*, 108004. [[CrossRef](#)]
25. Ding, R.S.; Kang, S.Z.; Zhang, Y.Q.; Hao, X.M.; Tong, L.; Du, T.S. Partitioning evapotranspiration into soil evaporation and transpiration using a modified dual crop coefficient model in irrigated maize field with ground-mulching. *Agric. Water Manag.* **2013**, *127*, 85–96. [[CrossRef](#)]
26. Yan, H.; Wu, H.; Zhang, C.; Acquah, S.; Zhao, B.; Huang, S. Estimation of greenhouse cucumber evapotranspiration in different seasons based on modified dual crop coefficient model. *Trans. Chin. Soc. Agric. Eng.* **2018**, *34*, 117–125.
27. Liu, G.; Du, Q.; Jiao, X.; Li, J. Irrigation at the level of evapotranspiration aids growth recovery and photosynthesis rate in tomato grown under chilling stress. *Acta Physiol. Plant.* **2017**, *40*, 2. [[CrossRef](#)]
28. Chen, N.; Li, X.; Shi, H.; Yan, J.; Hu, Q.; Zhang, Y. Modeling maize evapotranspiration and associated processes under biodegradable film mulching in an arid dripped field. *Agric. For. Meteorol.* **2021**, *297*, 10247. [[CrossRef](#)]
29. Chen, Z.; Sun, S.; Zhu, Z.; Jiang, H.; Zhang, X. Assessing the effects of plant density and plastic film mulch on maize evaporation and transpiration using dual crop coefficient approach. *Agric. Water Manag.* **2019**, *225*, 105765. [[CrossRef](#)]
30. Wang, Y.; Zou, Y.; Cai, H.; Zeng, Y.; He, J.; Yu, L.; Zhang, C.; Saddique, Q.; Peng, X.; Siddique, K.H.M.; et al. Seasonal variation and controlling factors of evapotranspiration over dry semi-humid cropland in guanzhong plain, china. *Agric. Water Manag.* **2022**, *259*, 107242. [[CrossRef](#)]
31. Zheng, J.; Fan, J.; Zhang, F.; Zhuang, Q. Evapotranspiration partitioning and water productivity of rainfed maize under contrasting mulching conditions in northwest china. *Agric. Water Manag.* **2021**, *243*, 106473. [[CrossRef](#)]
32. Granier, A.; Huc, R.; Barigah, S. Transpiration of natural rain forest and its dependence on climatic factors. *Agric. For. Meteorol.* **1996**, *78*, 19–29. [[CrossRef](#)]
33. Niu, Y.; Lyu, H.; Liu, X.; Zhang, M.; Li, H. Effects of supplemental lighting duration and matrix moisture on net photosynthetic rate of tomato plants under solar greenhouse in winter. *Comput. Electron. Agric.* **2022**, *198*, 107102. [[CrossRef](#)]
34. Danner, M.; Locherer, M.; Hank, T.; Richter, K. Measuring Leaf Area Index (LAI) with the LI-Cor LAI 2200C or LAI-2200 (+2200Clear Kit)—theory, measurement, problems, interpretation. In *EnMAP Field Guide Technical Report*; LI-Cor, Inc. Biosciences: Lincoln, NE, USA, 2015.
35. Chen, N.; Li, X.; Shi, H.; Hu, Q.; Zhang, Y.; Sun, Y.; Song, F. Simulation of maize crop growth using an improved crop model considering the disintegrated area of biodegradable film. *Field Crops Res.* **2021**, *272*, 108270. [[CrossRef](#)]
36. Ding, R.; Kang, S.; Li, F.; Zhang, Y.; Tong, L. Evapotranspiration measurement and estimation using modified priestley–taylor model in an irrigated maize field with mulching. *Agric. For. Meteorol.* **2013**, *168*, 140–148. [[CrossRef](#)]
37. Chen, Z.; Sun, S.; Wang, Y.; Wang, Q.; Zhang, X. Temporal convolution-network-based models for modeling maize evapotranspiration under mulched drip irrigation. *Comput. Electron. Agric.* **2020**, *169*, 105206. [[CrossRef](#)]
38. Steinberg, S.L.; Van Bavel, C.H.M.; McFarland, M.J. Improved sap flow gauge for woody and herbaceous plants. *Agron. J.* **1990**, *82*, 851–854. [[CrossRef](#)]
39. Gong, X.W.; Liu, H.; Sun, J.S.; Gao, Y.; Zhang, X.X.; Jha, S.K.; Zhang, H.; Ma, X.J.; Wang, W.N. A proposed surface resistance model for the penman-monteith formula to estimate evapotranspiration in a solar greenhouse. *J. Arid. Land* **2017**, *9*, 530–546. [[CrossRef](#)]
40. Fu, S.; Wei, X.; Wang, T.; Bai, Y. Effects of different water and fertilizer treatments on grapevine sap flow and water consumption characteristics. *Sci. Hortic.* **2022**, *304*, 111317. [[CrossRef](#)]

41. Fernández, M.D.; Bonachela, S.; Orgaz, F.; Thompson, R.; López, J.C.; Granados, M.R.; Gallardo, M.; Fereres, E. Measurement and estimation of plastic greenhouse reference evapotranspiration in a mediterranean climate. *Irrig. Sci.* **2010**, *28*, 497–509. [[CrossRef](#)]
42. Steduto, P.; Hsiao, T.C.; Raes, D.; Fereres, E. Aquacrop—The fao crop model to simulate yield response to water: I. Concepts and underlying principles. *Agron. J.* **2009**, *101*, 426–437. [[CrossRef](#)]
43. Fang, H.; Li, Y.; Gu, X.; Yu, M.; Du, Y.; Chen, P.; Li, Y. Evapotranspiration partitioning, water use efficiency, and maize yield under different film mulching and nitrogen application in northwest china. *Field Crops Res.* **2021**, *264*, 108103. [[CrossRef](#)]
44. Miao, Y.; Ren, J.; Zhang, Y.; Chen, X.; Qi, M.; Li, T.; Zhang, G.; Liu, Y. Effect of low root-zone temperature on photosynthesis, root structure and mineral element absorption of tomato seedlings. *Sci. Hortic.* **2023**, *315*, 111956.
45. Ntatsi, G.; Savvas, D.; Druerge, U.; Schwarz, D. Contribution of phytohormones in alleviating the impact of sub-optimal temperature stress on grafted tomato. *Sci. Hortic.* **2013**, *149*, 28–38. [[CrossRef](#)]
46. Agurla, S.; Gahir, S.; Munemasa, S.; Murata, Y.; Raghavendra, A.S. Mechanism of Stomatal Closure in Plants Exposed to Drought and Cold Stress. In *Survival Strategies in Extreme Cold and Desiccation*; Iwaya-Inoue, M., Sakurai, M., Uemura, M., Eds.; Advances in Experimental Medicine and Biology; Springer: Singapore, 2018; Volume 1081, pp. 215–232.
47. Vaten, A.; Bergmann, D.C. Mechanisms of stomatal development: An evolutionary view. *Evodevo* **2012**, *3*, 11. [[CrossRef](#)] [[PubMed](#)]
48. Zhang, K.; Kimball, J.S.; Kim, Y.; McDonald, K.C. Changing freeze-thaw seasons in northern high latitudes and associated influences on evapotranspiration. *Hydrol. Process.* **2011**, *25*, 4142–4151. [[CrossRef](#)]
49. Yang, P.; Hu, H.; Tian, F.; Zhang, Z.; Dai, C. Crop coefficient for cotton under plastic mulch and drip irrigation based on eddy covariance observation in an arid area of northwestern china. *Agric. Water Manag.* **2016**, *171*, 21–30. [[CrossRef](#)]
50. Amayreh, J.; Al-Abed, N. Developing crop coefficients for field-grown tomato (*Lycopersicon esculentum* mill.) under drip irrigation with black plastic mulch. *Agric. Water Manag.* **2005**, *73*, 247–254. [[CrossRef](#)]
51. Ding, R.S.; Tong, L.; Li, F.S.; Zhang, Y.Q.; Hao, X.M.; Kang, S.Z. Variations of crop coefficient and its influencing factors in an arid advective cropland of northwest china. *Hydrol. Process.* **2015**, *29*, 239–249. [[CrossRef](#)]
52. Jiao, L.J.; Ding, R.S.; Kang, S.Z.; Du, T.; Tong, L.; Li, S. A comparison of energy partitioning and evapotranspiration over closed maize and sparse grapevine canopies in northwest china. *Agric. Water Manag.* **2018**, *203*, 251–260. [[CrossRef](#)]
53. Gong, X.W.; Liu, H.; Sun, J.S.; Ma, X.J.; Wang, W.N.; Cui, Y.S. Modeling evapotranspiration of greenhouse tomato under different water conditions based on the dual crop coefficient method. *Ying Yong Sheng Tai Xue Bao J. Appl. Ecol.* **2017**, *28*, 1255–1264.
54. Jensen, C.R.; Orum, J.E.; Pedersen, S.M.; Andersen, M.N.; Plauborg, F.; Liu, F.; Jacobsen, S.E. A short overview of measures for securing water resources for irrigated crop production. *J. Agron. Crop Sci.* **2014**, *200*, 333–343. [[CrossRef](#)]
55. Mukherjee, A.; Kundu, M.; Sarkar, S. Role of irrigation and mulch on yield, evapotranspiration rate and water use pattern of tomato (*Lycopersicon esculentum* L.). *Agric. Water Manag.* **2010**, *98*, 182–189. [[CrossRef](#)]
56. Jafari, M.; Kamali, H.; Keshavarz, A.; Momeni, A. Estimation of evapotranspiration and crop coefficient of drip-irrigated orange trees under a semi-arid climate. *Agric. Water Manag.* **2021**, *248*, 106769. [[CrossRef](#)]
57. Fan, J.; Yue, W.; Wu, L.; Zhang, F.; Cai, H.; Wang, X.; Lu, X.; Xiang, Y. Evaluation of svm, elm and four tree-based ensemble models for predicting daily reference evapotranspiration using limited meteorological data in different climates of china. *Agric. For. Meteorol.* **2018**, *263*, 225–241. [[CrossRef](#)]
58. Patanè, C.; Tringali, S.; Sortino, O. Effects of deficit irrigation on biomass, yield, water productivity and fruit quality of processing tomato under semi-arid mediterranean climate conditions. *Sci. Hortic.* **2011**, *129*, 590–596. [[CrossRef](#)]
59. Santos, M.D.S.; Bomfim, G.V.d.; Azevedo, B.M.d.; Carvalho, A.C.P.d.; Fernandes, C.N.V. The production of ornamental pineapple in pots under different drip-irrigation depths. *Rev. Ceres* **2020**, *67*, 111–118. [[CrossRef](#)]
60. Hunsaker, D.J.; Bronson, K.F. Fao56 crop and water stress coefficients for cotton using subsurface drip irrigation in an arid us climate. *Agric. Water Manag.* **2021**, *252*, 106881. [[CrossRef](#)]
61. Jiang, S.; Liang, C.; Zhao, L.; Gong, D.; Huang, Y.; Xing, L.; Zhu, S.; Feng, Y.; Guo, L.; Cui, N. Energy and evapotranspiration partitioning over a humid region orchard: Field measurements and partitioning model comparisons. *J. Hydrol.* **2022**, *610*, 127890. [[CrossRef](#)]
62. Alberto, M.C.R.; Quilty, J.R.; Buresh, R.J.; Wassmann, R.; Haidar, S.; Correa, T.Q.; Sandro, J.M. Actual evapotranspiration and dual crop coefficients for dry-seeded rice and hybrid maize grown with overhead sprinkler irrigation. *Agric. Water Manag.* **2014**, *136*, 1–12. [[CrossRef](#)]

Disclaimer/Publisher’s Note: The statements, opinions and data contained in all publications are solely those of the individual author(s) and contributor(s) and not of MDPI and/or the editor(s). MDPI and/or the editor(s) disclaim responsibility for any injury to people or property resulting from any ideas, methods, instructions or products referred to in the content.